

Laminar Separation Bubble Effect on the Lift Curve Slope of an Airfoil

K. L. Hansen¹, R. M. Kelso¹, A. Choudhry¹ and M. Arjomandi¹

¹School of Mechanical Engineering
University of Adelaide, South Australia 5005, Australia

Abstract

This paper explores some unusual aerodynamic features that can arise due to the existence of laminar separation bubbles which occur at a transitional Reynolds number of 120,000 on two standard NACA airfoils of 21% thickness-to-chord ratio. These effects include an apparent increase in the lift-curve slope beyond the ideal lift slope ($2\pi \text{ rad}^{-1}$) at high angles of attack as well as a sudden stall characteristic. In addition, on one typical airfoil profile, it is demonstrated that negative lift can be generated at low angles of attack. In each case the laminar separation bubble is found to alter the curvature of the external flow, leading to an effective change in the camber of the foil.

Introduction

At low chordwise Reynolds numbers, particularly in the range of 70,000 to 200,000, the adverse pressure gradient on the low-pressure surface of airfoils can cause the laminar boundary layer to separate, transition to turbulence and then reattach to the surface at a downstream location, leading to formation of a laminar separation bubble [10]. This phenomenon is an important scale effect that must be understood by designers and researchers, especially since Reynolds numbers higher than 200,000 can only be obtained in relatively large and fast wind tunnels. Thus, an understanding of laminar separation bubbles is important to facilitate their analysis, identification and control.

Two standard NACA airfoils with 21% thickness-to-chord ratio were investigated in this study: NACA 0021 and NACA 65-021. These airfoils have different chordwise positions of maximum thickness which leads to variation in boundary layer and separation characteristics. For thick airfoil sections such as these, boundary layer separation typically initiates from the trailing edge and gradually progresses towards the leading edge with increasing angle of attack [1]. The stall characteristics are thus more gradual compared to thinner airfoil sections, where the separation initiates from the leading edge, causing a sudden loss in lift. Therefore, thick airfoils are desirable in applications where the wind speed can be variable such as the inflow conditions to wind turbine blades [7]. A more gradual stall characteristic gives rise to increased efficiency and reduced noise emissions under such conditions.

Experimental and Numerical Techniques

The airfoils used in the force measurements were modelled using a computer-aided drawing package and fabricated in aluminium using a programmable numerically controlled (NC) milling machine. A high quality surface finish was achieved on the models and the trailing edges were free from imperfections. The force measurements were undertaken in a closed working section that was attached to the contraction exit of a wind tunnel at the University of Adelaide. The wind tunnel has cross-sectional dimensions of 500 mm by 500 mm and the working section is 2400 mm in length. The Reynolds number was $Re = 120,000$, based on the freestream velocity of $U_\infty = 25\text{m/s}$ and the chord length of the airfoil. Lift and drag measurements were obtained using the 6-component load cell from JR3 which is accurate to

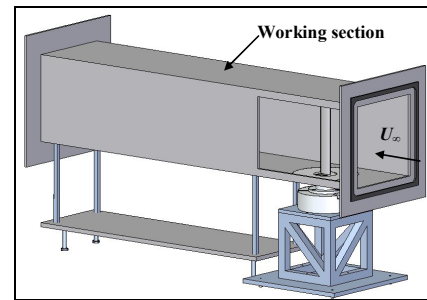


Figure 1: Drawing showing experimental set-up.

0.25%. The base of the load cell, as shown in Figure 1, consisted of a heavy steel plate to inhibit the effects of floor vibration and a stiff frame to minimize vibrational disturbances generated by the airflow. The angle of attack of the airfoil was set using a Vertex brand 200 mm diameter rotary table, which has a resolution of $\pm 0.2^\circ$. The angle of attack was increased only and therefore hysteresis effects were not investigated. The gap size between the airfoil wing tip and the working section ceiling was 3 mm, which was chosen to minimize three-dimensional effects whilst simultaneously allowing the airfoil to be conveniently mounted and rotated. This value is within the range of the suggested maximum gap of $0.005 \times \text{span}$ [2] required to avoid the effects of flow leakage around the tip.

To observe the surface pressures, static pressure ports were incorporated into the surfaces of the two airfoils under investigation. The small thickness of the airfoils increased the complexity of incorporating pressure taps into the existing models. Hence, it was decided that it would be more feasible to manufacture airfoils using a casting technique whereby the pressure taps could be moulded into the design during fabrication. Polyester resin was used as the casting material and strips of carbon fibre were distributed throughout the resin for strengthening and stiffening. The pressure tap tubes had an inner diameter of 1 mm and consisted of copper tubing inside the airfoil, followed by vinyl tubing.

The numerical simulations of the flow around a NACA 0021 airfoil were carried out using the commercial CFD software, ANSYS Fluent, Release 14.5. This software uses a cell-centred control volume space discretisation approach for the flow domain to solve the governing equations of the flow. The computational grid used in the simulation was constructed using POINTWISE and an O-type grid topology, centred on the airfoil, was implemented to minimise skewness of the near-wall elements. The grid boundaries were located 20 chord-lengths from the centre of the airfoil to ensure that the boundaries did not influence the flow. To verify that spatial discretisation errors were minimal, a grid independence study was conducted and it was shown that doubling the mesh density had negligible effect on the drag coefficient. The total number of elements used in the final mesh was 250,000 and 30 inflation layers were used to accurately model the boundary layer. The height of the first grid cell was based

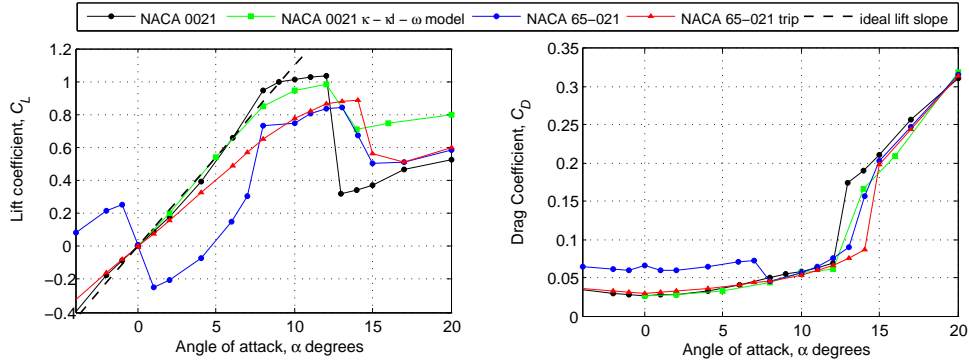


Figure 2: Comparison of lift and drag coefficients for NACA 0021 and NACA 65-021 at Reynolds number of 120,000.

on the minimum value of $y^+ \leq 1$, which is required by the low Reynolds number turbulent models used in this investigation to accurately model the boundary layer. The laminar kinetic energy ($\kappa - \kappa_l - \omega$) model used in the simulation was proposed by Walters and Cokljat [15] and is based on observations of the phenomena associated with laminar kinetic energy. The model improves predictions of the transition process by solving three additional transport equations for laminar and turbulent kinetic energy. The specific dissipation rate is also calculated along with the basic RANS equations. Further information pertaining to the numerical simulations can be found in Choudhry *et al.*[4]

Results

Force Measurements

The lift and drag results for a NACA 0021, NACA 65-021 and tripped NACA 65-021 are shown in Figure 2 and the ideal lift curve slope predicted by thin airfoil theory is included for comparison. The influence of the separation bubble is reflected in the variable slope of the lift coefficient against angle of attack plot corresponding to the untripped airfoils. The effect is less pronounced for the NACA 0021 airfoil and manifests in an increasing lift curve slope for $5 < \alpha < 8^\circ$, causing a slight exceedance of the theoretical lift slope. A similar increase in the lift curve slope between $5 < \alpha < 8^\circ$ is observed for the NACA 65-021 airfoil, although the amount of lift generated at these angles is far below the theoretical curve. Additionally, the presence of one or more separation bubbles has a significant consequence for the NACA 65-021 airfoil at angles of attack between $0 \leq \alpha \leq 4^\circ$. For these angles, a lift force is produced in the opposite direction to that expected for a symmetrical airfoil at a positive angle of attack as shown in Figure 2.

Further measurements indicated that the magnitude of the negative lift force is the same for both a clockwise and anti-clockwise rotation of the airfoil, which negates the possibility that the phenomenon was due to model asymmetry as suggested by Mueller and Batill [12]. These researchers noticed the same negative lift effect for a NACA 663-018 airfoil at $Re \approx 130,000$ but attributed it to surface irregularities resulting from a surface finish done by hand after milling. Marchaj [11] also observed negative lift generation where a comparison was made between a NACA 63-018 and a NACA 64-018 airfoil at $Re = 2,600,000$. It was found that the airfoil section with maximum thickness further aft (NACA 64-018) experienced negative lift characteristics, whereas the other airfoil section had a linear lift curve slope which passed through the origin. This author attributed the negative lift to a significant thickening of the boundary layer at the trailing edge on the top surface of the airfoil, leading to a larger effective curvature on the bottom surface of the airfoil relative to the top

surface and hence, negative lift.

The negative lift behaviour of the NACA 65-021 airfoil was ameliorated through use of 0.4 mm boundary layer trip tape placed on the suction and pressure surfaces. The height and position of the trips were optimised to give the lowest possible drag and maximum lift, while maintaining a linear relationship between C_L and α in the pre-stall regime. The roughness height, k , was first estimated according to the guidelines proposed by Braslow, Hicks and Harris [3] and then verified by experiment. The results in Figure 2 (NACA 65-021 trip) show that the trip is sufficient to eliminate all of the separation bubbles responsible for the negative lift and sudden lift increases and that the slope of the lift curve is approximately linear. Moreover, the drag of the NACA 65-021 airfoil is significantly reduced for all pre-stall angles of attack when a trip is used.

Figure 2 indicates that there is good agreement between the experimental and numerical results, particularly at low angles of attack. The numerically-derived lift coefficient begins to under-predict the measured value at approximately $\alpha = 8^\circ$, and this continues until the stall angle of 12 degrees. Both the numerical model and the experimental results indicate that stall occurs at this angle, however the experimentally measured stall is much more abrupt, resulting in a significant loss of lift. Post-stall, the numerical model over-predicts the amount of lift generated by the airfoil. The drag coefficient is well-predicted by the numerical model prior to the onset of stall, after which point the experimental results are under-predicted. These results suggest that the separation characteristics are not exactly captured by the numerical model, despite the fact that the model described herein, $\kappa - \kappa_l - \omega$, showed much better agreement than the $\gamma - Re_\theta$ model. Nonetheless, a slight increase in the lift coefficient slope is evident for the numerical results between between $5 < \alpha < 8^\circ$, which is consistent with the experimental results but somewhat less pronounced.

Surface Pressure Measurements

The pressure distribution data corresponding to the experimental results and numerical simulations for the NACA 0021 airfoil are shown in Figure 3 for selected pre-stall angles of attack. The existence of a separation bubble is reflected in both the experimental and numerical data and can be identified as the section of the suction curve where the pressure gradient starts to decrease, almost reaching a value of zero. After the separation bubble, the pressure gradient increases rapidly and then reaches the value which would be predicted in the absence of the separation bubble. The numerical model consistently under-predicts the pressures developed over the upper section of the airfoil, particularly at the low-pressure peak. On the other hand, there is good agreement

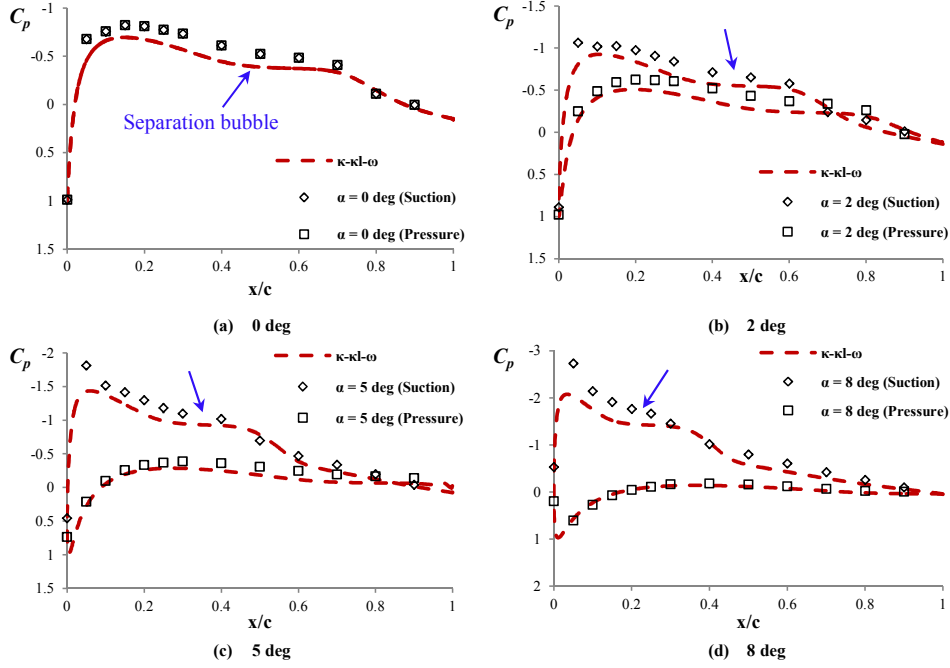


Figure 3: Comparison of pressure coefficient at selected angles of attack for the NACA 0021 airfoil at Reynolds number of 120,000.

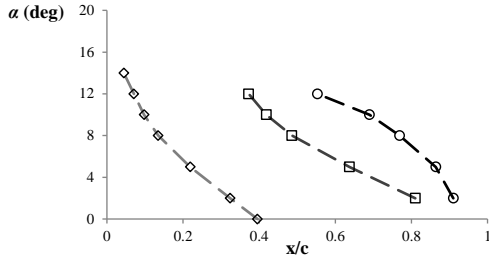


Figure 4: Location of the laminar separation (\diamond), turbulent reattachment (\square) and turbulent separation (\circ) on the NACA 0021 airfoil at a Reynolds number of 120,000.

between the experimental and numerical results for the pressure surface of the airfoil, demonstrating that the numerical model performs well for attached flows with small pressure gradients.

The exact location of the separation bubble is difficult to distinguish through observation of the surface pressure distributions alone and therefore, skin friction data were obtained from the numerical solution to fulfill this purpose. The results are shown in Figure 4. A separation bubble is predicted to occur on the suction surface for all angles of attack greater than $\alpha = 0^\circ$. With increasing angle of attack, the separation bubble moves towards the leading edge and there is a corresponding reduction in bubble length from $\alpha = 2^\circ$ to $\alpha = 12^\circ$.

The presence of the separation bubble gives rise to an increase in the apparent camber of the airfoil since it is large enough to cause the external flow to be diverted over the suction surface. As the bubble moves forward, there is an associated benefit of increased lift since an airfoil with maximum camber point close to leading edge develops a high maximum lift coefficient [13]. Hence at high angles of attack, the slope of the lift curve can exceed the theoretical maximum of $\kappa = 2\pi$ [13]. This anomaly can be explained in more detail through consideration of the lift coefficient for a cambered airfoil, given by Equation (1).

$$C_L = \kappa \left(\alpha + \frac{2h_{max}}{c} \right) \quad (1)$$

The amount of lift generated at a given angle of attack is governed by the camber, which is pictured in Figure 5. Therefore, the data points for an airfoil with variable camber exist on curves with differing values of $2h_{max}/c$. Connection of the data points corresponding to varying degrees of camber leads to an increasing lift curve slope as highlighted in Figure 6. A further implication of the presence of the separation bubble is the effect that it has on the stall characteristic of the NACA 0021 airfoil. The sudden loss in lift associated with the onset of stall can be explained by the “bursting” of the short separation bubble [8]. Generally, thick airfoils such as the NACA 0021 experience a more gradual stall since boundary layer separation is initiated from the trailing edge and gradually proceeds towards the leading edge as the angle of attack is increased [1]. However, when the boundary layer separation point is coincident with the edge of the separation bubble, the flow no longer reattaches. If the initial separation point is close to the leading edge then the airfoil immediately stalls, leading to a sudden loss in lift. Data for the NACA 0021 were collected by Jacobs [9] and also Swalwell and Sheridan [14] where it was observed that this airfoil stalled more gradually at higher Reynolds numbers and also for flow regimes with a higher turbulence intensity.

A similar investigation was carried out for the NACA 65-021 airfoil, although in this instance, data from the XFOIL analysis

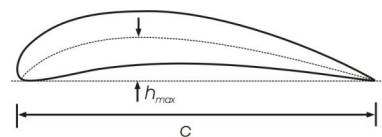


Figure 5: Sketch showing camber.

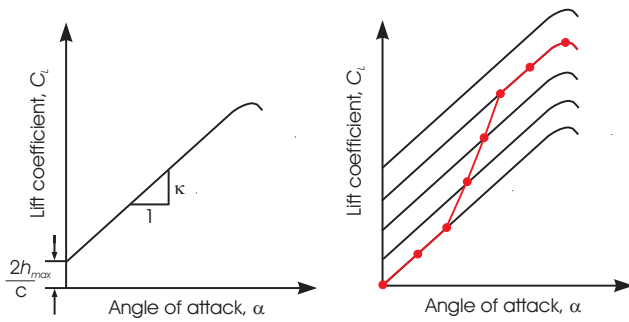


Figure 6: Explanation for increase in lift curve slope beyond theoretical maximum.

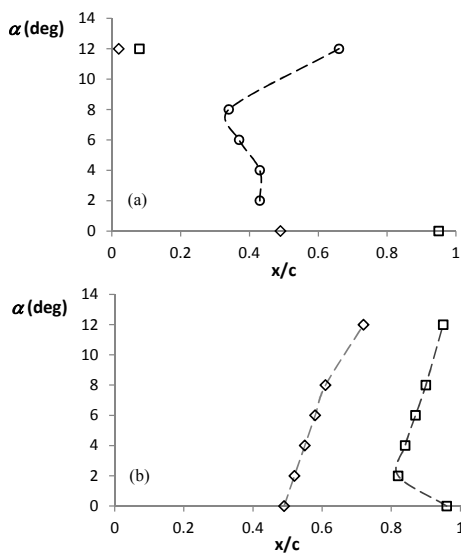


Figure 7: Location of the laminar separation (\diamond), turbulent reattachment (\square) and turbulent separation (\circ) points on (a) suction surface and (b) pressure surface of the NACA 65-021 airfoil at a Reynolds number of 120,000.

code [5] was used in the absence of CFD data for the NACA 65-021 airfoil. Surface pressure distribution data for the NACA 65-021 airfoil not shown here indicated reasonable agreement between the experimental and XFOIL results, which was also observed for the NACA 0021 airfoil[6]. To explain the negative lift phenomenon observed in the lift coefficient results for this airfoil, separation characteristics were examined on both the suction and pressure surfaces and the results are shown in Figure 7 (a) and (b), respectively.

The results indicate that a separation bubble consistently occurs on the pressure surface of the airfoil but only occurs on the suction surface at $\alpha = 0^\circ$ and $\alpha = 12^\circ$. In the latter case, the bubble is very short and would therefore have negligible impact on effective camber. On the other hand, the separation bubble on the pressure surface extends over 30% of the chord length for angles of attack up to $\alpha = 8^\circ$. Therefore, its presence increases the effective camber of the airfoil on the pressure surface, thus leading to negative lift generation at low angles of attack. The change from negative to positive lift occurs because the model asymmetry increases with angle of attack. At a certain point, $\alpha = 6^\circ$, the counterclockwise or positive circulation created by the separation bubble becomes less than the circulation created by model asymmetry which leads to overall negative circulation, which is required for positive lift generation. Use of boundary

layer trips on the NACA 65-021 airfoil eliminates the separation bubbles on the pressure surface thus eliminating the negative lift generating mechanism.

Conclusions

Laminar separation bubbles are an important scale effect that must be understood by designers and researchers as their presence can cause deterioration in the performance of an airfoil. At high angles of attack, when the suction-side laminar separation bubble has moved close to the leading edge, the apparent camber of a NACA 0021 airfoil is increased, thus allowing the airfoil to generate more lift than would be expected from the geometrical profile shape. At the point where the separation bubble “bursts”, there is a sudden loss in lift. The negative lift phenomenon observed for the NACA 65-021 airfoil is related to a pressure-side separation bubble which alters the effective camber on this surface. This effect persists until the angle of attack is sufficiently large that the pressure-side adverse pressure gradient disappears and positive lift is restored. Introducing surface roughness can effectively eliminate the observed anomalies in the lift curve slope, which further confirms that separation bubbles are responsible.

References

- [1] Anderson, J. D., *A history of aerodynamics and its impact on flying machines*, volume 8, Cambridge University Press, 1998.
- [2] Barlow, J., Rae, W. and Pope, A., *Low-speed wind tunnel testing*, John Wiley & Sons, Canada, 1999.
- [3] Braslow, A. L., Hicks, R. M. and Harris, R. V., *NASA TN D-3579*, volume 3579, National Aeronautics and Space Administration, 1966.
- [4] Choudhry, A., Arjomandi, M. and Kelso, R., A study of long separation bubble on thick airfoils and its consequent effects (submitted, 2014), *International Journal of Heat and Fluid Flow*.
- [5] Drela, M. and Youngren, H., *XFOIL 6.94 user guide*, Massachusetts Institute of Technology, Cambridge, MA, 2001.
- [6] Hansen, K. L., *Effect of leading edge tubercles on airfoil performance.*, PhD thesis, University of Adelaide, 2012.
- [7] Hansen, M. O., *Aerodynamics of wind turbines*, Routledge, 2013.
- [8] Hoerner, S. F. and Borst, H. V., *Fluid-dynamic lift: practical information on aerodynamic and hydrodynamic lift*, Hoerner Fluid Dynamics, Brick Town, NJ, 1985.
- [9] Jacobs, E. N., *The aerodynamic characteristics of eight very thick airfoils from tests in the variable density wind tunnel*, National Advisory Committee for Aeronautics, 1932.
- [10] Lissaman, P., Low-reynolds-number airfoils, *Annual Review of Fluid Mechanics*, **15**, 1983, 223–239.
- [11] Marchaj, C. A., *Aero-hydrodynamics of sailing*, Adlard Coles Nautical, 1991.
- [12] Mueller, T. J. and Batil, S. M., Experimental studies of separation on a two-dimensional airfoil at low reynolds numbers, *AIAA Journal*, **20**, 1982, 457–463.
- [13] Simons, M., *Model aircraft aerodynamics*, Nexus Special Interests Hemel Hempstead, UK, 2002.
- [14] Swalwell, K., Sheridan, J., Melbourne, W. et al., The effect of turbulence intensity on stall of the naca 0021 aerofoil, in *14th Australasian Fluid Mechanics Conference*, 2001, 941–944.
- [15] Walters, D. K. and Cokljat, D., A three-equation eddy-viscosity model for reynolds-averaged navier–stokes simulations of transitional flow, *Journal of Fluids Engineering*, **130**, 2008, 121401.